International Biodeterioration & Biodegradation 137 (2019) 88–94

Contents lists available at ScienceDirect

International Biodeterioration & Biodegradation

journal homepage: www.elsevier.com/locate/ibiod

Characterization of the catabolic pathway of diclofenac in *Raoultella* sp. KDF8

Andrea Palyzová, Jiří Zahradník, Helena Marešová, Tomáš Řezanka*

The Czech Academy of Sciences, Institute of Microbiology, Vídeňská 1083, 142 20, Prague 4, Czech Republic

ARTICLE INFO

Keywords:
Raoultella
Biodegradation
Diclofenac
Proteomics
Metabolomics

ABSTRACT

The removal of diclofenac, which is a widely used non-steroidal anti-inflammatory drug and a dangerous environmental contaminant of surface water, was studied. Its complete degradation by *Raoultella* sp. KDF8 to primary metabolic products was described with individual metabolites identified by mass spectrometry. The *Raoultella* strain KDF8 was cultivated with unlabelled and ^{13}C6-labelled diclofenac. A total of 32 compounds were detected as intermediates in diclofenac metabolism by high resolution tandem mass spectrometry. Furthermore, proteomic analysis showed that the presence of diclofenac resulted in the upregulation of 24 enzymes associated with the benzoate, catechol, protocatechuate and ketoadipate pathways. The presence of genes encoding specific enzymes, such as catechol 1,2-dioxygenase, protocatechuate 3,4-dioxygenase and quercetin 2,3-dioxygenase, has been verified by sequence analysis of PCR products. The description of diclofenac metabolism by strain KDF8 provides a detailed view of the degradation of xenobiotic aromatic compounds by microorganisms in general.

1. Introduction

Diclofenac (2-[2-[(2,6-dichlorophenyl)amino]phenyl]acetic acid; DCF), which is an anti-inflammatory drug, shows considerable consumption, widespread use and a consequent presence in the environment (Duan et al., 2013). This pollutant is associated with the vulture crisis in India and Pakistan (Oaks et al., 2004), has a high environmental risk worldwide (Hernando et al., 2006) and was included as a priority substance in the watch list for union-wide monitoring up to 2018 (Commission implementing decision 2015/495/EU). The presence of DCF is frequently detected in wastewater treatment plant (WWTP) influents and effluents (concentration range μg L^{-1}, Metcalfe et al., 2004), and in surface water (ng L^{-1}, Wiegel et al., 2004). Conventional WWTPs have a limited ability to remove these compounds during water treatment. It is known that biodegradation of DCF by activated sludge is not sufficiently effective (Pereira et al., 2015).

Despite vast knowledge on the distribution of analgesics in the environment, very little is known about their fates, especially in terms of their microbial co-metabolism or biotransformation (Liu et al., 2001). DCF has been found to be degradable in soils (Al-Rajab et al., 2010), but the relevant organisms have not been identified. Degraders (bacteria and fungi) have been mainly isolated from the sludge of WWTPs and soil contaminated by the drug. The efficient degradation of DCF (75%) at an initial concentration of 300 mg L^{-1} within three weeks was described using a microbial consortium of activated sludge (Langenhoff et al., 2013). Batch degradation processes were conducted with activated sludge in a membrane bioreactor where DCF was removed by up to 40% after 18 days and the degradation rate remained stable during batch incubation (Bouju et al., 2016). In addition, data on the toxicity of DCF and the ability to remove this drug by the bacterial strain *Raoultella* sp. DD4 was reported by Domaradzka et al. (2016). Another strain, *Raoultella* sp. KDF8, was reported to be resistant to high concentrations of DCF (up to 3.0 g L^{-1}), but the compound could not be used as a source of carbon and energy by the strain (Palyzová et al., 2018). This strain was capable of removing DCF efficiently (97%) after 48 h in co-metabolism with ethanol. Moreira et al. (2018) reported a 70% biodegradation of DCF (1.7–34 μM) by the bacterial strain *Labrys portucalensis* F11 via co-metabolism with acetate.

The metabolism of DCF in humans and animals has been extensively studied. The first mention of the biotransformation of DCF sodium salt in animals and humans was provided by Riess et al. (1976). Enzymatic hydroxylation of micronutrients, including DCF in mammals and some microorganisms, is often carried out by cytochrome P450, laccases and peroxidases (Domaradzka et al., 2015) to form the major hydroxylated derivatives of 4′-hydroxy and 5-hydroxy metabolites (Prior et al., 2010; Sparidans et al., 2008; Shen et al., 1999) and the minor metabolites 3′-

* Corresponding author.
E-mail address: rezanka@biomed.cas.cz (T. Řezanka).

https://doi.org/10.1016/j.ibiod.2018.11.013
Received 10 September 2018; Received in revised form 26 November 2018; Accepted 26 November 2018

hydroxy-diclofenac, 4′-hydroxy-diclofenac sulphate and 4′,5-dihydroxy-diclofenac (Stierlin et al., 1979). Gröning et al. (2007) showed that under aerobic conditions, biofilms of river sediment extensively transformed DCF to *p*-benzoquinone imine of 5-hydroxy-diclofenac, which was not further degraded, in an apparent co-metabolic process. Stable carbon isotopes have been employed to identify strategies for biological degradation. This approach was used to assess the fate of DCF during degradation by *Trametes versicolor* (Badia-Fabregat et al., 2014).

Even though DCF degradation has been intensively studied, many important aspects are still missing. The aim of this study was to investigate the proteomic and metabolomic backgrounds of the possible pathways of DCF degradation by the fully characterized bacterial strain *Raoultella* sp. KDF8 (Palyzová et al., 2018) using at carbon stable isotope.

2. Materials and methods

2.1. Chemicals and materials

The standards of the molecules 2-[(2,6-dichlorophenyl)amino]phenylacetic acid sodium salt (DCF), [2-(2,6-dichlorophenylamino) phenyl^{13}C6]acetic acid sodium salt hemi(nonahydrate) (^{13}C6 DCF) and 4′-hydroxy-diclofenac were purchased from Sigma-Aldrich (St. Louis, MO, USA). The other chemicals and ingredients (high analytical grade) were obtained from Merck (Kenilworth, NJ, USA) and Sigma-Aldrich.

2.2. Microorganism and culture conditions

The strain *Raoultella* sp. KDF8 (CCM 8678) was obtained by the chemical mutagenesis (Palyzová et al., 2018) of a bacterial isolate from polluted soil. Luria-Bertani (LB) medium (in g L^{-1}: tryptone 10, yeast extract 5 and NaCl 10) was used to prepare pre-inoculum cultures of the strain (10 mL cultures shaken for 24 h at 28 °C at 200 rpm). Degradation of DCF was studied in Basal salt broth (BSB) medium (in g L^{-1}: NaCl 0.1, K_2HPO_4 1.03, KH_2PO_4 0.75, and NH_4Cl 1) supplemented with trace elements (in mg L^{-1}: $MgSO_4.7H_2O$ 200, $CaCl_2.2H_2O$ 10, $ZnSO_4.7H_2O$ 6.6, $MnSO_4.H_2O$ 0.17, $FeSO_4.7H_2O$ 1.5, $CoCl_2.6H_2O$ 0.48, $CuSO_4.5H_2O$ 0.47, and $Na_2MoO_4.2H_2O$ 0.45; BSBTE). In the proteomic study (culturing for 48 h), 10 mL of BSBTE medium was supplemented with glycerol (1.0 g L^{-1}) or DCF (1.0 g L^{-1}). Metabolomic studies (culturing for 72 h) were performed in 10 mL of BSBTE medium supplemented with DCF or ^{13}C6 DCF at concentrations of 1.0 g L^{-1}. The cultures (in duplicate) were inoculated with pelleted biomass from precultures washed by BSB medium. The cultures were incubated at 28 °C and 200 rpm. To prepare stock solutions of DCF and ^{13}C6 DCF (100 mg mL^{-1}), the compound was dissolved in ethanol.

2.3. Analysis of DCF metabolites by shotgun mass spectrometry

The strain *Raoultella* sp. KDF8 was cultivated in BSBTE medium with DCF or ^{13}C6-DCF. The intermediates of the DCF co-metabolic pathway were extracted from culture supernatants as follows: a 0.5 mL sample was extracted with 0.5 mL of TBME under vigorous shaking on a vortex mixer (3 mL vials, vortex mixer, and 10 min). The organic and water phases were separated by centrifugation (12 000 × *g* for 10 min). The organic phases were used for high-resolution electrospray ionization-mass spectrometry (HRESI).

An LTQ-Orbitrap Velos mass spectrometer (Thermo Fisher Scientific, San Jose, CA, USA) equipped with a heated electrospray interface (HESI) was operated in positive and negative ionization mode. The MS scan range was performed in the FT cell and recorded within a window between 100 and 1000 *m/z*. The mass resolution was set to 105 000, and the ion spray voltage was set at 3.5 kV (in the positive ionization mode) and − 2.5 kV (in the negative ionization mode). Both ionization modes used the following parameters: sheath gas flow, 18 arbitrary units (AU); auxiliary gas flow, 7 AU; ion source temperature, 250 °C; capillary temperature, 230 °C; capillary voltage, 50 V; and tube lens voltage, 170 V. Helium was used as a collision gas for collision-induced dissociation (CID) experiments. The CID normalization energy of 35% was used for the fragmentation of parent ions.

The calibration of the MS spectrometer was conducted with the use of a Pierce LTQ Orbitrap positive and/or negative ion calibration solution (Thermo Fisher Scientific, San Jose, CA, USA). The internal lock mass was used in mass spectra acquisition, i.e., 255.2330 *m/z* $[M-H]^-$ palmitic acid in the negative ESI. The mass accuracy was better than 2 ppm. The chemical structure of the compounds was confirmed with the help of the spectral database Metlin (https://metlin.scripps.edu/).

2.4. Protein extraction and LC-MS analysis

The culture biomasses in the exponential (24 h) and stationary (48 h) phases of growth were harvested by centrifugation (5 min, 8000 × *g*, and 4 °C), washed and resuspended by phosphate-buffered saline buffer (PBS, 137 mM NaCl, 2.7 mM KCl, 10 mM Na_2HPO_4, and 1.8 mM KH_2PO_4) to obtain a 10% w/v suspension. The samples were sonicated with the addition of sodium deoxycholate to a final concentration of 2%. The protein concentrations were determined by using a Pierce™ BCA Protein Assay Kit (Thermo Fisher Scientific, San Jose, CA, USA). Cysteines in the samples (200 µg of proteins) were reduced with 5 mM tris-(2-carboxyethyl) phosphine (TCEP, 60 °C, and 60 min) and blocked by 10 mM methyl methanethiosulfonate (MMTS, 10 min, and 25 °C). Pretreated samples of the proteins were digested by trypsin (1:100 ratio, overnight, and 37 °C) and desalted on a C18 column (Hichrom Ltd., Reading, Berks, UK).

For peptide analysis, the samples were applied on nLC-MS with a trap column (Acclaim PepMap 300, C18, 5 µm, 300 Å, and 300 µm × 5 mm) and a nano reversed-phase separation column (EASY-Spray column, C18, 2 µm, 100 Å, and 75 µm × 50 cm). The liquid chromatography protocol (a flow rate of 15 µL min^{-1}, buffer A: 2% acetonitrile, 0.1% formic acid and buffer B: 80% acetonitrile, 0.1% formic acid) consisted of the 3 steps: sample application for 4 min, linear gradient 2–40% buffer B for 60 min, and 90% buffer B for 8 min.

2.5. Gel-free comparative proteomics experiments with LC/MS Q-TOF and data processing

Eluted peptides were directly ionized by electrospray and analysed on a Thermo Orbitrap Fusion mass spectrometer (Q-OT-qIT, Thermo Fisher Scientific, San Jose, CA, USA). Peptide precursors from 400 to 1600 *m/z* (120 K resolution and 200 *m/z*) were trapped and those with charge states 2–6 were sampled for MS/MS. The dynamic exclusion duration was set to 45 s with a 10 ppm tolerance. The spectra were acquired using an activation time of 30 ms and normalized collision energy of 30. The instrument was set to top speed mode with 2 s cycles.

All data were processed using label-free algorithms in MaxQuant (version 1.5.3.8) and Andromeda software (for MS/MS data) (Cox et al., 2011). The acquired data were used to search for the *Raoultella ornithinolytica* protein sequences in a database (NCBI non-redundant protein sequences, 7631 sequences, July 2016). Dithiomethylation, oxidation of methionines and protein N-terminal acetylation were defined as variable modifications. The maximum false discovery rate (FDR) was set to 1% for peptide spectral matches of proteins. The final data were analysed using Perseus software (Tyanova et al., 2016) (threshold p-value 0.05) and further revised, inferred and manually sorted. The spectral count for individual LC-MS/MS runs was also recorded. Changes in protein abundance were calculated via a direct comparison between the mean peak intensity of five replicates of the sample and the control. The raw mass spectrometry proteomics data have been deposited in the ProteomeXchange Consortium via the PRIDE (Vizcaíno et al., 2016) partner repository with the dataset identifier PXD010643 and the processed proteomics data have been deposited in the Zenodo repository (Zahradník and Palyzová, 2017; http://doi.org/10.5281/zenodo.579575).

Table 1
Primers used for amplification and sequencing of *Raoultella* sp.KDF8 genes.

Gene	Primer	Sequence	Targed size (bp)
Protocatechuate 3,4-dioxygenase	fwd PCTD	5′-AATGATAAATGGTCACCGCGCG- 3′	1359
	rew PCTD	5′-TCAGATATCAAAGAAGACGGTTTCGTTCTCACCC- 3′	
Catechol 1,2-dioxygenase	fwd CATD	5′-AAAAATTCTTTCGTACAACAAGAAGCCG- 3′	927
	rev CATD	5′-TTACTCTTGTGCGCGCAGGCGGG- 3′	
Quercetin 2,3-dioxygenase	fwd QED	5′-ATCTACTTACGCAAAGCTAATGAACGCGG- 3′	696
	rev QED	5′-TCAGACCGGCGGCAGATCG- 3′	

2.6. PCR amplification of the catechol 1,2-dioxygenase, protocatechuate 3,4-dioxygenase and quercetin 2,3-dioxygenase

The genomic DNA of *Raoultella* sp. KDF8 was isolated with the High Pure PCR Template Preparation Kit (Roche, Mannheim, Germany) and was used as a template for the amplification of the protocatechuate 3,4-dioxygenase (PCTD), catechol 1,2-dioxygenase (CATD) and quercetin 2,3-dioxygenase (QED) genes. Specific primers were designed from the genomic sequence of *R. ornithinolytica* B6 (Table 1). A standard three-step PCR protocol was performed using Q5 High-Fidelity DNA Polymerase (New England Biolabs. Inc, Ipswich, MA, USA) as follows: 5 min at 94 °C followed by 35 cycles of denaturation at 94 °C for 30 s; annealing for 45 s at temperatures 69 °C, 67 °C and 72 °C for PCTD, CATD and QED, respectively; amplification at 72 °C for 1 min and a final extension period of 5 min at 72 °C. The purified PCR products were subjected to direct sequencing using the BigDye Terminator v 3.1 Cycle Sequencing Kit (Applied Biosystems, Foster City, CA, USA) on an Applied Biosystems 3130xl Genetic Analyzer. The nucleotide sequences of all of the fragments were compared with the GenBank NCBI database (BLASTN 2.8.0 program).

3. Results

3.1. Determination of metabolites during DCF degradation

Shotgun analysis on the LTQ Orbitrap Velos was used to detect and identify biodegradation products by HRESI mass spectrometry. Due to the complexity of the biodegradation samples, this unique approach allowed for a great deal of information for essentially all of the metabolites (chemical compounds) from moderately polar to non-polar. To eliminate the interference of compounds that are not DCF biodegradation products, we first used unlabelled DCF and/or labelled DCF (^{13}C6-DCF) as a carbon source in the parallel cultivation of *Raoultella* sp. KDF8 (see Section 2.2). Additionally, the detection of biodegradation products was facilitated by the characteristic isotope profile of the molecules containing two chlorine atoms (neutral loss scan [M-H−H^{35}Cl]$^-$ and [M-H−H^{37}Cl]$^-$ in an abundance of ions in the ratio ~3:1). In the case of bacterial cultivation with labelled-DCF (^{13}C6-DCF), the ions with an unusually high content of ^{13}C were identified by MS/MS. Fig. 1 shows the negative HRESI mass spectra of standards ^{13}C6-DCF, unlabelled DCF and 4′-hydroxy-diclofenac in the interval of molecular ions.

The ions of the compounds extracted from cells cultured with unlabelled and labelled DCF (DCF versus ^{13}C6-DCF), i.e., differing by multiples of 1.00335 Da (difference between atomic weights ^{12}C and ^{13}C) and between ^{35}Cl and ^{37}Cl (a difference of 1.997 Da), were obtained for detection and identification. The results of the analyses show the presence of nearly 32 biodegradation intermediates of DCF and ^{13}C6-DCF. Namely, 18 compounds retained the structure of the core of the DCF molecule (Table 2) and 14 compounds had structures indicating subsequent DCF secondary amine bond cleavage (Tables 2 and 3). Two products that are DCF building blocks, i.e., hydroxy-phenyl-acetic acid and 2,6-dichloroaniline derivatives, were identified by MS/MS (Table 4). Some of the identified hydroxy-phenyl-acetic acid derivatives can be further used as sources of carbon and energy in the primary metabolism of bacterial cells.

Biodegradation pathways have been revealed using labelled and unlabelled DCF and with three major hydroxylated diclofenacs (5-hydroxy-diclofenac, M-1; 6-hydroxy-diclofenac, M-2; and 4′-hydroxy-diclofenac, M-3) as parent compounds. An increase of 16 Da relative to the parent molecule was observed, indicating mono-hydroxylated DCF. The presence of abundant ions in the mass spectrum of M-1 (at *m/z* 266.0149) and M-3 (at *m/z* 266.0131) confirmed that these molecules

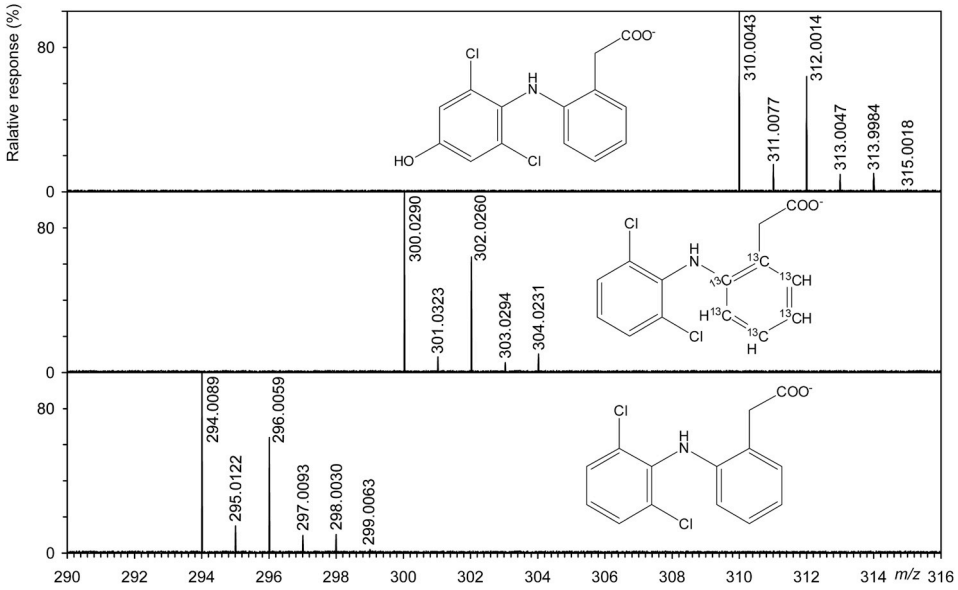

Fig. 1. HRESI mass spectra of 4′-hydroxy-diclofenac, ^{13}C6-DCF and unlabelled DCF.

Table 2
Overview of the metabolites found during the degradation of DCF determined by accurate mass measurements and the elemental composition.

Metabolite *m/z*	Measured	Mass error (ppm)	Elemental composition	References
M-1	310.0037	0.6	$C_{14}H_{11}Cl_2NO_3$	Marco-Urrea et al. (2010)
M-2	310.0039	0.4	$C_{14}H_{11}Cl_2NO_3$	This study
M-3	310.0036	0.7	$C_{14}H_{11}Cl_2NO_3$	Marco-Urrea et al. (2010)
M-4	307.9873	1.4	$C_{14}H_9Cl_2NO_3$	Groning et al. (2007); Kosjek et al. (2008)
M-5	279.9929	0.9	$C_{13}H_9Cl_2NO_2$	Moreira et al. (2018)
M-6	295.9876	1.1	$C_{13}H_9Cl_2NO_3$	Moreira et al. (2018)
M-7	311.9830	0.6	$C_{13}H_9Cl_2NO_4$	Moreira et al. (2018)
M-8	324.0183	1.7	$C_{15}H_{13}Cl_2NO_3$	This study
M-9	325.9974	1.8	$C_{14}H_{11}Cl_2NO_4$	This study
M-10	323.9816	2.0	$C_{14}H_9Cl_2NO_4$	This study
M-11	295.9878	0.9	$C_{13}H_9Cl_2NO_3$	This study
M-12	311.9832	0.4	$C_{13}H_9Cl_2NO_4$	This study
M-13	327.9770	1.5	$C_{13}H_9Cl_2NO_5$	This study
M-14	266.0123	2.2	$C_{13}H_{11}Cl_2NO$	This study
M-15	325.9986	0.6	$C_{14}H_{11}Cl_2NO_4$	This study
M-16	341.9938	0.4	$C_{14}H_{11}Cl_2NO_5$	This study
M-17	357.9877	1.4	$C_{14}H_{11}Cl_2NO_6$	This study
M-18	355.9723	1.1	$C_{14}H_9Cl_2NO_6$	This study
M-19	151.0377	2.4	$C_8H_8O_3$	This study
M-20	191.9622	0.3	$C_6H_5Cl_2NO_2$	This study
M-21	192.9457	0.8	$C_6H_4Cl_2O_3$	This study

Table 3
A list of metabolites containing carbon stable isotopes of labelled diclofenac (^{13}C6-DCF) produced during degradation by *Raoultella* sp. KDF8.

Metabolite	Measured m/z	Mass error (ppm)	Elemental composition
M-22	173.0537	1.4	$C_2{}^{13}C_6\ H_8O_4$
M-23	176.0439	2.8	$C_2{}^{13}C_5\ H_8O_5$
M-24	192.0400	1.6	$C_2{}^{13}C_5\ H_8O_6$
M-25	190.0249	1.0	$C_2{}^{13}C_5H_6O_6$
M-26	148.0234	0.9	$C_2{}^{13}C_3\ H_6O_5$
M-27	130.0116	2.1	$C_2{}^{13}C_3H_4O_4$
M-28	134.0434	1.6	$C_2{}^{13}C_3\ H_8O_4$
M-29	134.0354	0.7	$^{13}C_5\ H_7O_4$
M-30	152.0456	1.1	$^{13}C_5\ H_8O_5$
M-31	150.0287	2.3	$^{13}C_5\ H_6O_5$
M-32	106.0119	1.8	$^{13}C_3H_4O_4$

Table 4
Measurement of the MS/MS product ion spectra of the key metabolites formed during DCF degradation.

Metabolite	Products MS/MS m/z (abundance in %)
M-1	266.0149 (100); 230.0362 (58); 215.0138 (6); 194.0595 (31); 166.0650 (24)
M-2	266.0197 (100); 230.0428 (29); 215.0185 (6); 194.0643(13); 192.0454 (38); 187.0209 (12); 166.0686 (2); 123.9986 (5)
M-3	268.0292 (17); 266.0131 (100); 263.9983 (19); 135.0442 (53); 117.0328 (7)
M-7	312.0184 (6); 293.9971 (48); 266.1221 (84); 230.0378 (100)
M-8	256.0160 (41); 220.0393 (45); 192.4440 (100)
M-10	251.9977 (25); 235.0395 (14); 216.0211 (37); 134.9760 (5); 132.9610 (15); 108,0455 (86)
M-14	230.0371 (45); 194.0577 (61); 166.0641 (100)
M-15	310.0038 (17); 266.0116 (17); 231.0433 (100); 230.0354 (61); 196.0733 (2); 195.0667 (3)
M-16	235.0395 (14); 180.0444 (49); 133.0284 (100); 150.0552 (22)
M-19	135.0422 (9); 128.0806 (3); 107.0490 (100)
M-20	156.9931 (100); 139.9903 (58)
M-21	157.9771 (100); 140.9743 (61)

were identified as hydroxylated diclofenacs [2-(2-((2,6-dichlorophenyl) amino)-5-hydroxyphenyl)acetic acid] and [2-(2-((2,6-dichloro-4-hydroxyphenyl)amino)phenyl)acetic acid]. Methylation of the hydroxyl group of M-1 has been proposed by the presence of an ion at *m/z* 192.4440 (M-8) in MS/MS spectra, i.e., the $[M\text{-}H]^-$ of 14 Da was higher than that of M-1. The M-7 metabolite was formed from hydroxylated

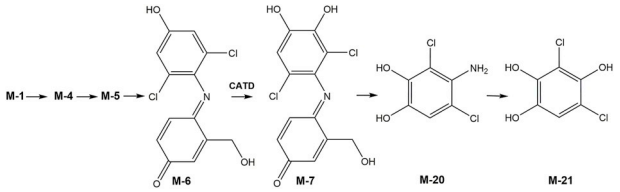

Fig. 2. Putative degradation pathway of compound M-1 via catechol 1,2-dioxygenase (CATD) attack: (*E*)-4-((2,6-dichloro-4-hydroxyphenyl)imino) -3-(hydroxymethyl)cyclohexa-2,5-dien-1-one (M-6), (*E*)-(6-((2,6-dichloro-3,4-dihydroxyphenyl)imino)-3-oxocyclohexa-1,4-dien-1-yl)methanolate (M-7), 4-amino-3,5-dichlorobenzene-1,2-diol (M-20), and 3,5-dichlorobenzene-1,2,4-triol (M-21).

diclofenac (M-1) by a series of reactions involving the hydroxylation and oxidation of the aromatic skeleton including the side chain. Another reaction leading to the M-20 metabolite and then to M-21 is the cleavage of a very stable p-quinone derivative and the exchange of the amino group (M-20) with the hydroxyl (M-21); see Fig. 2.

The detection of ions at *m/z* 194.0643 observed in the mass spectrum of M-2 provided evidence that hydroxylation occurred on a non-chlorinated ring (Table 4). The metabolite was identified as 6-hydroxy-diclofenac [2-(2-((2,6-dichlorophenyl)amino)-6-hydroxyphenyl)acetic acid]. The M-2 molecule is the parental structure for the formation of mono-hydroxylated (M-9, 10, 11), di-hydroxylated (M-12) and tri-hydroxylated (M-13) DCF products (Table 2). The structure of the M-10 metabolite was confirmed by MS/MS in which the ions listed in Table 4 were identified. These are ions resulting from the elimination of simple stable molecules such as HCl and CO_2.

The biodegradation pathway, which starts from the molecule M-3, revealed a 44 Da decrease of $[M\text{-}H]^-$ in M-14 and indicated decarboxylation (loss of −COOH group) from molecule M-3 (Table 2). M-15 represents the elimination of the three neutral molecules, which indicates that the carboxyl group and two atoms of chlorine were present (Fig. 3). Thus, two hydroxyls were identified from the M-15 molecule, which corresponded to an increase in the $[M\text{-}H]^-$ value by 32 Da (two oxygen). The structure of the M-16 metabolite was again based on MS/MS; see Table 4. In this case, the ions resulting from the splitting of the aromatic ring (originally substituted by two atoms of chloride) are present in the spectrum. Again, in MS/MS, ions were formed by the loss of small neutral molecules, i.e., CO_2, H_2O, and HCl.

Another DCF biodegradation pathway that produces primary metabolites of the bacterial cell was identified only by means of labelled

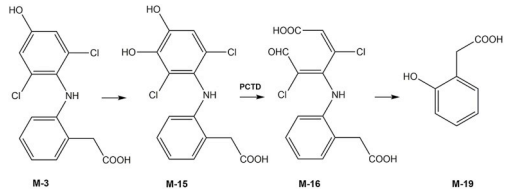

Fig. 3. Putative degradation pathway of compound M-3 via protocatechuate 3,4-dioxygenase (PCTD) attack: 2-(2-((2,6-dichloro-3,4-dihydroxyphenyl) amino)phenyl)acetic acid ((M-15), 2-(2-(((1*E*,3*Z*)-1-carboxy-2,4-dichloro-5-oxopenta-1,3-dien-3-yl)amino)phenyl)acetic acid (M-16), and 2-(2-hydroxyphenyl)acetic acid (M-19).

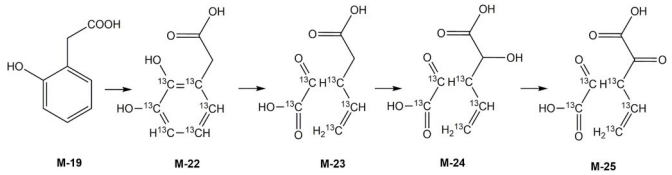

Fig. 4. Identified metabolites and their position in the putative degradation pathway of compound M-19: 2-(2,3-dihydroxyphenyl)acetic acid (M-22), 3-(carboxycarbonyl)pent-4-enoic acid (M-23), 3-(carboxycarbonyl)-2-hydroxypent-4-enoic acid (M-24), and 3-(carboxycarbonyl)-2-oxopent-4-enoic acid (M-25).

DCF from hydroxy-phenyl acetic acid (M-19; Fig. 4). The M-19 metabolite was further oxidized to the compound dihydroxy-phenyl acetic acid (M-22). In addition, the primary metabolites, for example, malonic, oxoglutaric, 3-hydroxyglutaric, and hydroxy-oxo-valeric acids (M-26–M-32), that resulted from sequential oxidations during the degradation pathway were identified. Only the compounds M-22 to M-32 containing a ring with six atoms of ^{13}C are shown in Table 3 as representatives of ^{13}C-containing compounds. Splitting the benzene ring was the critical point of biodegradation; subsequent biodegradation products (M-23–M-32) were rapidly metabolized and their identification was performed by negative HRESI on the basis of the $[M\text{-}H]^-$ ions containing non-natural abundance of ^{13}C isotopes.

3.2. Diclofenac degradation - associated proteome

A comparative proteomic study was performed to identify pathways involved in diclofenac degradation, and proteins further associated with its metabolism. We analysed two independent samples of each culture. The first sampling was performed after 24 h in the exponential phase of growth and the second sample was obtained after 48 h from the stationary glycerol culture and the declining phase of growth of the DCF culture. The study identified numerous proteins that were differentially expressed in the cells grown in the DCF- and glycerol-supplemented medium. In total, we identified 2523 different proteins that correspond to approximately 51% coverage of the theoretical proteome (the reference genome of *R. ornithinolytica* B6 encodes 4909 genes). After data processing, we analysed 1995 proteins from the first sampling and 2044 proteins from the second sampling. In total, 412 proteins were significantly overrepresented (more than a 2-fold change) in the sample after 24 h and 319 were significantly overrepresented in the sample after 48 h of growth. In addition, we also identified 158 significantly underrepresented proteins (less than 0.5-fold change) in the sample of DCF-grown cells after 24 h and 199 underrepresented proteins after 48 h (data not shown). Based on the shotgun proteomic analysis, we identified 24 upregulated, intracellular proteins in DCF-grown cells when compared to glycerol-grown cells, which may be involved in the DCF degradation pathway. All of the identified proteins are listed in Table 5. These proteins were further grouped according to their participation in the metabolic pathways for: benzoate degradation (clusters designated

Table 5
Putative proteins involved in diclofenac degradation.

Protein name	GenBank ID	Cluster[a]	Fold change	
			24 h[b]	48 h
Phenylacetic acid-responsive transcriptional repressor PaaX family	AGJ86189.1	Phenyl acetate^A	0.87	0.76
Phenylacetate-CoA ligase	AGJ86190.1	Phenyl acetate^A	0.9	0.63
4-hydroxyphenylacetate catabolism protein	AGJ87785.1	Phenyl acetate^B	1.98	0.91
3,4-dihydroxyphenylacetate 2,3-dioxygenase	AGJ87788.1	Phenyl acetate^B	0.7	0.22
4-hydroxyphenylacetate 3-monooxygenase reductase subunit	AGJ87795.1	Phenyl acetate^B	OFF	ON
Catechol 1,2-dioxygenase	AGJ86048.1	Catechol	4.21	1.5
Muconolactone isomerase	AGJ86049.1	Catechol	1.71	0.88
Muconate and chloromuconate cycloisomerase	AGJ86050.1	Catechol	ON	ND
Pca regulon regulatory protein PcaR	AGJ86051.1	Catechol	ON	ND
Aminobenzoyl-glutamate transporter	AGJ85755.1	Benzoate	ON	ON
Aminobenzoyl-glutamate utilization protein B	AGJ85756.1	Benzoate	6.84	4.23
Aminobenzoyl-glutamate utilization protein	AGJ85757.1	Benzoate	6.94	36.-46
Pca regulon regulátory protein PcaR	AGJ85760.1	Benzoate	1.1	1.0
3-oxoadipate CoA-transferase subunit A	AGJ85761.1	Benzoate	ON	ND
2,3-dihydroxybenzoate-2,3-dehydrogenase	AGJ87084.1	Benzoate	1.58	1.33
Hypothetical protein RORB6_07275	AGJ86146.1	Catechuate	2.94	2.14
Protocatechuate 3,4-dioxygenase subunit beta	AGJ86147.1	Catechuate	ON	ON
Protocatechuate 3,4-dioxygenase subunit alpha	AGJ86148.1	Catechuate	ON	ON
LysR family transcriptional regulator YdcI	AGJ86149.1	Catechuate	2.49	1.23
Oxidoreductase	AGJ88763.1	Quercetin	1.09	1.25
Quercetin 2,3-dioxygenase	AGJ88764.1	Quercetin	ND	1.02
Beta-ketoadipyl CoA thiolase	AGJ86191.1		ON	ON
Succinyl-CoA:3-ketoacid-coenzyme A transferase subunit B	AGJ85619.1		ON	ON
Succinyl-CoA synthetase subunit beta	AGJ86969.1		2.43	2.00

[a] Clusters were identified by searching for co-localization of genes for up-represented proteins identified by MS in a genome of reference strain *R. ornithinolytica* B6. Subsequently significantly up-represented or down-represented neighboring genes were taken into account. The upper index (A and B) is used to separate different genomic co-localization.

[b] ON – the protein presence was confirmed exclusively in the sample supplemented with DCF; OFF – the protein was detected only in the sample supplemented with glycerol; ND – the corresponding change cannot be determined due to the absence of data or it has been excluded from the dataset due to low statistical significance.

AGJ85755.1 - AGJ85766.1 also as a catechol degradation cluster AGJ86044.1 - AGJ86055.1), genes associated with protocatechuate 3,4-dioxygenase (AGJ86146.1 - AGJ86149.1), oxidoreductase (AGJ88763.1) and quercetin 2,3-dioxygenase (AGJ88764.1).

The sequence analysis of the PCR products obtained with specific primers for PCTD, CATD and QED further confirmed the presence of the genes encoding these key metabolic enzymes in the genome of the strain KDF8 (Fig. S1). The sequences are part of the whole genome shotgun sequence of strain KDF8 deposited at the DDBJ/ENA/GenBank under the accession number RCIX01000000. Homology analysis of all three sequences showed high nucleotide identity (> 98%) with genes encoding protocatechuate 3,4-dioxygenase, catechol 1,2-dioxygenase and quercetin 2,3-dioxygenase of *R. ornithinolytica* strains.

4. Discussion

Pathways for the degradation of diclofenac by microorganisms are intensively studied because the drug, as an environmental pollutant, represents a serious threat to living organisms. Critical DCF metabolic steps, which have not yet been solved follow the cleavage of at least one of the aromatic rings. This issue is not confined to the biodegradation of DCF but is valid for the biodegradation of all aromatic compounds. Since we used the labelled DCF (^{13}C6-DCF) in this study, the fate of the benzene ring containing 6 atoms of ^{13}C that is not substituted by two atoms of chloride was at least partially elucidated. The degradation of DCF predominantly occurred by hydroxylation reactions: three isomers were identified as 5- and 4′-hydroxy-diclofenac and 6-hydroxy-diclofenac. These metabolites were previously described during the degradation of DCF by fungi (Hata et al., 2010; Marco-Urrea et al., 2010), bacteria (Moreira et al., 2018; Domaradzka et al., 2015; Osorio-Lozada et al., 2008), a consortium of bacteria and fungi from river sediment (Gröning et al., 2007), or sludge from a sewage treatment plant (Kosjek et al., 2009). Commonly, the enzymatic hydroxylation reaction is the first step of the degradation of all aromatic compounds by mono- or dioxygenases (Prior et al., 2010; Seo et al., 2009), and the strain *Raoultella* sp. KDF8 is not an exception. Based on our proteomic data, we hypothesize that the DCF building block degradation is driven by dioxygenases. In our analysed proteomes, we did not identify over-represented cytochrome P450 enzymes, which have been reported in the oxidative metabolism of DCF (Klenk et al., 2017; Xu et al., 2015; Wester et al., 2003; Shen et al., 1999). In contrast, the upregulation of catechol 1,2-dioxygenase and protocatechuate 3,4-dioxygenase was confirmed in the degradation proteome, and structural genes were identified in the *Raoultella* sp. KDF8 genome by specific PCR and sequencing.

As shown in Table 2, further degradation of the hydroxylated metabolites may vary: most of them demonstrate preservation of the core of the diclofenac structure (Stylianou et al., 2018; Moreira et al., 2018). Methylation of the hydroxyl group of 5-hydroxy-diclofenac by the putative methyltransferase resulted in the formation of M-8 through a similar mechanism as that described in humans (Blum et al., 1996). The hydroxylation of α-substituted acetic acid of 6-hydroxy-diclofenac resulted in M-9 and the oxidation of the hydroxyl group of M-9 to keto (oxo)-acid (M-10) yielding M-11 after oxidative decarboxylation. A similar shortening of the side chain of M-4 to a compound missing one methylene group, i.e., a decarboxylation reaction of the aliphatic side chain and another oxidation step, was also previously reported (Faber et al., 2014; Coelho et al., 2009; Pérez-Estrada et al., 2005). Another hydroxylation M-5 with monooxygenase led to the formation of M-6 and subsequently to M-7. According to our hypothesis, another assigned compound formed by this metabolic pathway contains a benzoquinone imine structure, which is indicated by the formation of M-5 (Table 2). These structures (from M-4 to M-7) have been reported as products of microbial DCF transformation by Moreira et al. (2018).

Degradation pathways of aromatics involve oxidation reactions that are catalysed by mono- or dioxygenases to convert these compounds to dihydroxy aromatic intermediates (Cao et al., 2009). The dihydroxy compounds are subjected to ring cleavage using dioxygenases or other enzymes to form Krebs intermediate products (Seo et al., 2009). These types of cleavages were observed during DCF molecule degradation. Based on the results of the metabolomics, we identified an intradiol cleavage reaction between M-15 and M-16 and an extradiol cleavage between the compounds M-22 and M-23. The key role of the intradiol dioxygenases (catechol 1,2 and protocatechuate-3,4) in aromatic compound degradation was described by Guzik et al. (2013), and these enzymes were also identified by our proteomic analysis. The enzyme responsible for the extradiol cleavage was not observed in our proteomics data although its action is evident from the metabolomics data. Our proteomics results indicate the up-representation of proteins encoded by the quercetin dioxygenase cluster. The quercetin 2,3-dioxygenase catalyses the cleavage of the O-heteroaromatic ring of the flavonol quercetin (Balogh-Hergovich et al., 2000) and its role in the degradation of diclofenac is unclear. The next dioxygenase identified by proteomics was 3,4-dihydroxyphenylacetate 2,3-dioxygenase. The lower upregulation of this enzyme in the sample with DCF probably implies that it has no role in the degradation pathway.

Interestingly, phenylacetic acid was not degraded by the phenylacetic acid degradation pathway, which was revealed by the downregulation of the corresponding enzymes in the proteomic analysis (Table 5). The use of ^{13}C6 DCF with the labelled hydroxylphenylacetic acid ring enabled us to detect the metabolites, indicating the presence of the benzoate pathway. The presence of this pathway was further supported by the upregulation of beta-ketoadipyl CoA thiolase and the enzymes involved in succinyl-CoA metabolism (Table 5). The degradation of the 2,6-dichloroaniline fragment of the DCF molecule comprised oxidative cleavage of the benzene ring and the formation of the corresponding aminobenzene-diol (M-20). This product, 2,6-dichloro-3,4-hydroxy aniline, has been identified in the metabolome (Table 2; Fig. 2). The enzymes most likely responsible for this activity were described as 2-chlorobenzoate 1,2-dioxygenase (AGJ86045.1 and AGJ86046.1; Shin et al., 2013) and catechol 1,2-dioxygenase (AGJ86048.1; Table 5).

5. Conclusion

Our work deals with diclofenac metabolism by the bacterial strain *Raoultella* sp. KDF8. To describe the metabolic pathway of DCF, proteomic and metabolomic studies were included. This report uses the combination of these techniques and of ^{13}C-labelled diclofenac. This methodological approach allowed us to detect and identify products of the cleavage of the aromatic moieties of the DCF molecule up to primary metabolic products. For degradation of diclofenac, the strain uses metabolic pathways starting with hydroxylation reactions to form three major isomers of DCF molecule that are finally converted into products entering the Krebs cycle. It can be inferred from the identified metabolites and upregulated enzymes in DCF-replete medium that the KDF8 strain is capable of using a pathway combining catechol 1,2-dioxygenase and protocatechuate 3,4-dioxygenase for oxidation of both biphenyl rings. This innovative approach to the characterization of diclofenac degradation metabolism by the KDF8 strain provides a detailed insight into the degradation of xenobiotic aromatic compounds by microorganisms in general.

Acknowledgments

The research was supported by the Ministry of Education, Youth and Sports of the Czech Republic (LO1509) and the Epsilon programme (TH02030337) of the Technology Agency of the Czech Republic.

Appendix A. Supplementary data

Supplementary data to this article can be found online at https://doi.org/10.1016/j.ibiod.2018.11.013.

References

Al-Rajab, A.J., Sabourin, L., Lapen, D.R., Topp, E., 2010. The non-steroidal anti-inflammatory drug diclofenac is readily biodegradable in agricultural soils. Sci. Total Environ. 409, 78–82. https://doi.org/10.1016/J.SCITOTENV.2010.09.020.

Badia-Fabregat, M., Rosell, M., Caminal, G., Vicent, T., Marco-Urrea, E., 2014. Use of stable isotope probing to assess the fate of emerging contaminants degraded by white-rot fungus. Chemosphere 103, 336–342. https://doi.org/10.1016/J.CHEMOSPHERE.2013.12.029.

Balogh-Hergovich, E., Kaizer, J., Speier, G., 2000. Kinetics and mechanism of the Cu(I) and Cu(II) flavonolate-catalyzed oxygenation of flavonol. Functional quercetin 2,3-dioxygenase models. J. Mol. Catal. Chem. 159, 215–224. https://doi.org/10.1016/S1381-1169(00)00247-8.

Blum, W., Faigle, J.W., Pfaar, U., Sallmann, A., 1996. Characterization of a novel diclofenac metabolite in human urine by capillary gas chromatography-negative chemical ionization mass spectrometry. J. Chromatogr. B Biomed. Sci. Appl. 685, 251–263. https://doi.org/10.1016/S0378-4347(96)00198-3.

Bouju, H., Nastold, P., Beck, B., Hollender, J., Corvini, P.F.-X., Wintgens, T., 2016. Elucidation of biotransformation of diclofenac and 4′hydroxydiclofenac during biological wastewater treatment. J. Hazard Mater. 301, 443–452. https://doi.org/10.1016/J.JHAZMAT.2015.08.054.

Cao, B., Nagarajan, K., Loh, K.C., 2009. Biodegradation of aromatic compounds: current status and opportunities for biomolecular approaches. Appl. Microbiol. Biotechnol. 85, 207–228. https://doi.org/10.1007/s00253-009-2192–4.

Coelho, A.D., Sans, C., Agüera, A., Gómez, M.J., Esplugas, S., Dezotti, M., 2009. Effects of ozone pre-treatment on diclofenac: intermediates, biodegradability and toxicity assessment. Sci. Total Environ. 407, 3572–3578. https://doi.org/10.1016/J.SCITOTENV.2009.01.013.

Commission Implementing Decision (EU) 2015/495 of 20 March, 2015. Establishing a watch list of substances for Union-wide monitoring in the field of water policy pursuant to Directive 2008/105/EC of the European Parliament and of the Council. Official Journal C311/8, 25/10/2013. http://data.europa.eu/eli/dec_impl/2015/495/oj.

Cox, J., Neuhauser, N., Michalski, A., Scheltema, R.A., Olsen, J.V., Mann, M., 2011. Andromeda: a peptide search engine integrated into the MaxQuant environment. J. Proteome Res. 10, 1794–1805. https://doi.org/10.1021/pr101065j.

Domaradzka, D., Guzik, U., Hupert-Kocurek, K., Wojcieszyńska, D., 2016. Toxicity of diclofenac and its biotransformation by *Raoultella* sp. DD4. Polish. J. Environ. Stud. 25, 2211–2216. https://doi.org/10.15244/pjoes/62681.

Domaradzka, D., Guzik, U., Wojcieszyńska, D., 2015. Biodegradation and biotransformation of polycyclic non-steroidal anti-inflammatory drugs. Rev. Environ. Sci. Biotechnol. 14, 229–239. https://doi.org/10.1007/s11157-015-9364-8.

Duan, Y.P., Meng, X.Z., Wen, Z.H., Ke, R.H., Chen, L., 2013. Multi-phase partitioning, ecological risk and fate of acidic pharmaceuticals in a wastewater receiving river: the role of colloids. Sci. Total Environ. 447, 267–273. https://doi.org/10.1016/j.scitotenv.2013.01.017.

Faber, H., Lutze, H., Lareo, P.L., Frensemeier, L., Vogel, M., Schmidt, T.C., Karst, U., 2014. Liquid chromatography/mass spectrometry to study oxidative degradation of environmentally relevant pharmaceuticals by electrochemistry and ozonation. J. Chromatogr. A 1343, 152–159. https://doi.org/10.1016/J.CHROMA.2014.03.081.

Gröning, J., Held, C., Garten, C., Claußnitzer, U., Kaschabek, S.R., Schlömann, M., 2007. Transformation of diclofenac by the indigenous microflora of river sediments and identification of a major intermediate. Chemosphere 69, 509–516. https://doi.org/10.1016/J.CHEMOSPHERE.2007.03.037.

Guzik, U., Hupert-Kocurek, K., Wojcieszysk, D., 2013. Intradiol dioxygenases – the key enzymes in xenobiotics degradation. In: Chamy, R., Rosenkranz, F. (Eds.), Biodegradation of Hazardous and Special Products. InTech, London, pp. 129–153. https://doi.org/10.5772/56205.

Hata, T., Kawai, S., Okamura, H., Nishida, T., 2010. Removal of diclofenac and mefenamic acid by the white rot fungus *Phanerochaete sordida* YK-624 and identification of their metabolites after fungal transformation. Biodegradation 21, 681–689. https://doi.org/10.1007/s10532-010-9334-3.

Hernando, M.D., Heath, E., Petrovic, M., Barceló, D., 2006. Trace-level determination of pharmaceutical residues by LC-MS/MS in natural and treated waters. A pilot-survey study. Anal. Bioanal. Chem. 385, 985–991. https://doi.org/10.1007/s00216-006-0394-5.

Klenk, J.M., Nebel, B.A., Porter, J.L., Kulig, J.K., Hussain, S.A., Richter, S.M., Tavanti, M., Turner, N.J., Hayes, M.A., Hauer, B., Flitsch, S.L., 2017. The self-sufficient P450 RhF expressed in a whole cell system selectively catalyses the 5-hydroxylation of diclofenac. Biotechnol. J. 12, 1600520. https://doi.org/10.1002/biot.201600520.

Kosjek, T., Andersen, H.R., Kompare, B., Ledin, A., Heath, E., 2009. Fate of carbamazepine during water treatment. Environ. Sci. Technol. 43, 6256–6261. https://doi.org/10.1021/es900070h.

Langenhoff, A., Inderfurth, N., Veuskens, T., Schraa, G., Blokland, M., Kujawa-Roeleveld, K., Rijnaarts, H., 2013. Microbial removal of the pharmaceutical compounds ibuprofen and diclofenac from wastewater. BioMed Res. Int. 9 2013. https://doi.org/10.1155/2013/325806.

Liu, C.Y., Speitel, G.E., Georgiou, G., 2001. Kinetics of methyl t-butyl ether cometabolism at low concentrations by pure cultures of butane-degrading bacteria. Appl. Environ. Microbiol. 67, 2197–2201. https://doi.org/10.1128/AEM.67.5.2197-2201.2001.

Marco-Urrea, E., Pérez-Trujillo, M., Cruz-Morató, C., Caminal, G., Vicent, T., 2010. White-rot fungus-mediated degradation of the analgesic ketoprofen and identification of intermediates by HPLC–DAD–MS and NMR. Chemosphere 78, 474–481. https://doi.org/10.1016/J.CHEMOSPHERE.2009.10.009.

Metcalfe, C., Miao, X.-S., Hua, W., Letcher, R., Servos, M., 2004. Pharmaceuticals in the canadian environment. In: Kümmerer, K. (Ed.), Pharmaceuticals in the Environment. Springer Berlin Heidelberg, pp. 67–90. https://doi.org/10.1007/978-3-662-09259-0_6.

Moreira, I.S., Bessa, V.S., Murgolo, S., Piccirillo, C., Mascolo, G., Castro, P.M.L., 2018. Biodegradation of diclofenac by the bacterial strain *Labrys portucalensis* F11. Ecotoxicol. Environ. Saf. 152, 104–113. https://doi.org/10.1016/j.ecoenv.2018.01.040.

Oaks, J.L., Gilbert, M., Virani, M.Z., Watson, R.T., Meteyer, C.U., Rideout, B.A., Shivaprasad, H.L., Ahmed, S., Chaudhry, M.J.I., Arshad, M., Mahmood, S., Ali, A., Khan, A.A., 2004. Diclofenac residues as the cause of vulture population decline in Pakistan. Nature 247, 630–633. https://doi.org/10.1038/nature02317.

Osorio-Lozada, A., Surapaneni, S., Skiles, G.L., Subramanian, R., 2008. Biosynthesis of drug metabolites using microbes in hollow fiber cartridge reactors: case study of diclofenac metabolism by actinoplanes species. Drug Metab. Dispos. 36, 234–240. https://doi.org/10.1124/dmd.107.019323.

Palyzová, A., Zahradník, J., Marešová, H., Sokolová, L., Kyslíková, E., Grulich, M., Štěpánek, V., Řezanka, T., Kyslík, P., 2018. Potential of the strain *Raoultella* sp. KDF8 for removal of analgesics. Folia Microbiol. 63, 273–282. https://doi.org/10.1007/s12223-017-0563-2.

Pereira, A.M.P.T., Silva, L.J.G., Meisel, L.M., Lino, C.M., Pena, A., 2015. Environmental impact of pharmaceuticals from Portuguese wastewaters: geographical and seasonal occurrence, removal and risk assessment. Environ. Res. 136, 108–119. https://doi.org/10.1016/j.envres.2014.09.041.

Pérez-Estrada, L.A., Malato, S., Gernjak, W., Agüera, A., Thurman, E.M., Ferrer, I., Fernández-Alba, A.R., 2005. Photo-fenton degradation of diclofenac: identification of main intermediates and degradation pathway. Environ. Sci. Technol. 39, 8300–8306. https://doi.org/10.1021/es050794n.

Prior, J.E., Shokati, T., Christians, U., Gill, R.T., 2010. Identification and characterization of a bacterial cytochrome P450 for the metabolism of diclofenac. Appl. Microbiol. Biotechnol. 85, 625–633. https://doi.org/10.1007/s00253-009-2135-0.

Riess, W., Stierlin, H., Geiger, U.P., Gerardin, A., Schmid, K., Wagner, J., Theobald, W., 1976. Data on the pharmacokinetics and metabolism of Diclofenac (Voltaren) in animals and man. In: Wagenhäuser, F.J. (Ed.), Chronic Forms or Polyarthritis. Berne, Stuttgart and Vienna Huber, pp. 302–317.

Seo, J.S., Keum, Y.S., Li, Q.X., 2009. Bacterial degradation of aromatic compounds. Int. J. Environ. Res. Publ. Health 6, 278–309. https://doi.org/10.3390/ijerph6010278.

Shen, S., Marchick, M.R., Davis, M.R., Doss, G.A., Pohl, L.R., 1999. Metabolic activation of diclofenac by human cytochrome P450 3A4: role of 5-Hydroxydiclofenac. Chem. Res. Toxicol. 12, 214–222. https://doi.org/DOI:10.1021/tx9802365.

Shin, S.H., Um, Y., Beak, J.H., Kim, S., Lee, S., Oh, M.-K., Kim, Y.-R., Lee, J., Yang, K.-S., 2013. Complete genome sequence of *Raoultella ornithinolytica* strain B6, a 2,3-butanediol-producing bacterium isolated from oil-contaminated soil. Genome Announc. 1 e00395-13. https://doi.org/10.1128/genomeA.00395-13.

Sparidans, R.W., Lagas, J.S., Schinkel, A.H., Schellens, J.H.M., Beijnen, J.H., 2008. Liquid chromatography–tandem mass spectrometric assay for diclofenac and three primary metabolites in mouse plasma. J. Chromatogr. B 872, 77–82. https://doi.org/10.1016/J.JCHROMB.2008.07.012.

Stierlin, H., Faigle, J.W., Sallmann, A., Kung, W., Richter, W.J., Kriemler, H.-P., Alt, K.O., Winkler, T., 1979. Biotransformation of diclofenac sodium (Voltaren®) in animals and in man. Xenobiotica 9, 601–610. https://doi.org/10.3109/00498257909042327.

Stylianou, K., Hapeshi, E., Vasquez, M.I., Fatta-Kassinos, D., Vyrides, I., 2018. Diclofenac biodegradation by newly isolated *Klebsiella* sp. KSC: microbial intermediates and ecotoxicological assessment. J. Environ. Chem. Eng. 6, 3242–3248. https://doi.org/10.1016/J.JECE.2018.04.052.

Tyanova, S., Temu, T., Sinitcyn, P., Carlson, A., Hein, M.Y., Geiger, T., Mann, M., Cox, J., 2016. The Perseus computational platform for comprehensive analysis of (prote) omics data. Nat. Methods 13, 731–740. https://doi.org/10.1038/nmeth.3901.

Vizcaíno, J.A., Csordas, A., Del-Toro, N., Dianes, J.A., Griss, J., Lavidas, I., Mayer, G., Perez-Riverol, Y., Reisinger, F., Ternent, T., Xu, Q.W., Wang, R., Hermjakob, H., 2016. 2016 update of the PRIDE database and its related tools. Nucleic Acids Res. 44, D447–D456. https://doi.org/10.1093/nar/gkv1145.

Wester, M.R., Johnson, E.F., Marques-Soares, C., Dijols, S., Dansette, P.M., Mansuy, D., Stout, C.D., 2003. Structure of mammalian cytochrome P450 2C5 complexed with diclofenac at 2.1 Å resolution: evidence for an induced fit model of substrate binding. Biochemistry 42, 9335–9345. https://doi.org/10.1021/bi034556l.

Wiegel, S., Aulinger, A., Brockmeyer, R., Harms, H., Löffler, J., Reincke, H., Schmidt, R., Stachel, B., von Tümpling, W., Wanke, A., 2004. Pharmaceuticals in the river Elbe and its tributaries. Chemosphere 57, 107–126. https://doi.org/10.1016/J.CHEMOSPHERE.2004.05.017.

Xu, L.H., Ikeda, H., Liu, L., Arakawa, T., Wakagi, T., Shoun, H., Fushinobu, S., 2015. Structural basis for the 4′-hydroxylation of diclofenac by a microbial cytochrome P450 monooxygenase. Appl. Microbiol. Biotechnol. 99, 3081–3091. https://doi.org/10.1007/s00253-014-6148-y.

Zahradník, J., Palyzová, A., 2017. *Raoultella* sp. KDF8 proteome data. Zenodo. http://doi.org/10.5281/zenodo.579575.